

# GemNet: Analysis and Prediction of Building Materials for Optimizing Indoor Wireless Networks

Zhijin Yang\*, Zhizhen Li\*, Yi Wang\*, Jianqing Liu\*, Mingzhe Chen†, and Yuchen Liu\*

\*North Carolina State University, USA, †University of Miami, USA

**Abstract**—This paper investigates the correlation between building material properties and indoor network coverage, encompassing both indoor Wi-Fi and outdoor 5G technologies to provide customized network services tailored to users' needs in diverse areas. We first analyze the impact of building material characteristics, with a special focus on wall materials, on the distribution of wireless signal propagation. Then, a ray-tracing-based method is introduced to synthetically generate high-quality training data that covers fine-grained network scenarios with a wide range of wall materials, extending beyond traditional materials. This dataset serves as the foundation for our proposed Global Embedding Isomorphism Network (GemNet), a machine learning framework that facilitates the prediction of optimal material parameters for customized in-building coverage. This innovation enables architects and builders to design novel, network-friendly materials, ensuring ubiquitous and on-demand network services. Extensive evaluations consistently demonstrate a remarkable prediction accuracy of 90.52% on material parameters, underscoring the framework's ability to optimize indoor wireless network planning through the lens of material engineering.

## I. INTRODUCTION

As the reliance on internet resources continues to escalate, the necessity for advanced wireless connectivity in local area network (LAN) environments, inundated with various edge devices and Internet of Things (IoT) devices, becomes increasingly paramount. In this context, Wi-Fi technology, particularly in high-frequency bands such as 60 GHz, becomes indispensable for emerging bandwidth-hungry applications indoors. While 5G cellular network technology remains dominant for outdoor uses, it also plays a significant role in various indoor settings such as corporate offices, healthcare facilities, eateries, and industrial complexes. This is often due to private Wi-Fi access restrictions and security concerns. As illustrated in Fig. 1, some users or visitors opt to connect to 5G base stations (BS) to ensure uninterrupted real-time connectivity. This highlights 5G as a vital complementary technology for indoor applications, and it is anticipated that Wi-Fi and 5G technologies will collaborate synergistically to advance intelligent indoor network services [1]–[3].

In a typical indoor environment, Wi-Fi access points (APs) and 5G BSs can provide complementary coverage, allowing customized network services tailored to users' needs in various areas. However, it is crucial to emphasize that the choice of building construction materials, particularly wall materials, can significantly impact the transmission characteristics of signals emanating from 5G and Wi-Fi infrastructure. For instance, the wall materials with high transmittance properties facilitate the effective penetration of external 5G radio signals, while indoor Wi-Fi signals may experience increased dispersion in

such scenarios, and vice versa. As a result, the selection of optimal building materials becomes paramount in ensuring robustness and customized wireless coverage within indoor spaces. Specifically, the permittivity and conductivity of wall materials have a direct impact on the radio channel characteristics. For example, tinted windows with low conductivity, primarily designed to block ultraviolet light, can inadvertently obstruct RF signals from penetrating the building. This also results in noticeable variations in indoor coverage maps across different frequency bands, such as sub-6 GHz and 60 GHz, due to the distinctive permittivity and conductivity of the materials involved. As such, it is evident that there exists a substantial interplay between radio frequency bands, building material properties, and the distribution of wireless signals within the architectural structure.



Fig. 1: An integrated cellular-WiFi indoor network scenario.

Although research in the material engineering field, such as [4], [5], has explored the impact of building materials on wireless signal propagation through measurement campaigns, they focus solely on classical materials like brick and concrete, which limits the scope of studies for an optimal network planning. Other works such as [6]–[9] have specialized in material designs within the energy conservation and structure diversity domains. In terms of in-building coverage predictions, [10] concentrated on indoor millimeter-wave networks while neglecting enhancements for outdoor 5G technology. Despite machine learning techniques being utilized to estimate wall material properties, as seen in [7]–[9], [11], the potential of graph neural network (GNN) based models, capable of capturing the spatial correlation of wireless signals, remains underexplored in predicting building material properties for optimizing network coverage, which highlights a promising avenue for our research herein.

In practice, the interrelationship among the aforementioned three factors is intricate, dynamic, and potentially nonlinear. This complexity presents analytical challenges in customizing in-building coverage based on a variety of construction material parameters and cross-technology communication. To address this, we first conduct a comprehensive analysis of how various material parameters affect wireless coverage in integrated cellular-WiFi networks. Leveraging the effectiveness and accuracy of graph modeling for wireless networks, we then introduce *GemNet*, a material-inspired network planning framework, designed to optimize wireless coverage by selecting appropriate building materials. The main contributions of this work are summarized as follows:

- We perform a comprehensive analysis to understand how wireless signals are sensitive to building material properties. Notably, our findings indicate that modifying wall material characteristics, such as conductivity and permittivity, can have a positive effect on indoor network coverage with the cross-technology communication.
- We develop for the first time a ray-tracing-based method to synthetically generate high-quality training data covering fine-grained network scenarios that correlate a wide range of wall materials, which is then used to develop a graph isomorphism network learning framework, empowering the prediction of optimal material parameters for customized network coverage. This enables builders to design novel, network-friendly materials, ensuring ubiquitous and on-demand network services.
- We extensively evaluate our *GemNet* framework for predicting material parameters to achieve customized in-building coverage. The results consistently demonstrate an accuracy exceeding 90%, showcasing the framework's ability to accurately predict material parameters using detailed environmental information and characteristics of hybrid 5G and Wi-Fi signals.

## II. MOTIVATION AND ANALYSIS

With the proliferation of mobile and bandwidth-hungry applications, the need for ubiquitous wireless connectivity in both residential and professional environments has experienced a substantial surge. Consequently, recent study has been dedicated to enhancing Wi-Fi signal strength to achieve extensive coverage. Nonetheless, it is undeniable that wireless signal propagation invariably encounters indoor propagation challenges. Signal obstructions, often arising from physical barriers, result in “blind spots” within the space. Rather than rigidly pursuing comprehensive Wi-Fi coverage, an alternative approach is to take a holistic perspective, considering indoor Wi-Fi signals alongside the additional potential provided by outdoor 5G signals to address in-building coverage on demand.

To this end, we initiate an experimental study examining the impact of various wall materials on the distribution of 5G and Wi-Fi signals (sub-6 GHz and 60 GHz) within an indoor scenario. Fig. 2 shows the evaluation results from a high-fidelity ray-tracing software *Wireless Insite*®. By altering the material of the left outer wall, as illustrated in Fig. 1, it becomes evident that the received signal strength (RSS)

distribution maps for 5G and Wi-Fi differ, despite being within the same scenario. This variance arises due to the elevated transmission power of 5G BS and their longer wavelengths in comparison to Wi-Fi signals, which endow outdoor 5G signals with a more uniform RSS distribution owing to their enhanced penetration capabilities. In contrast, the high-band Wi-Fi signal strengths exhibit greater variability, being notably near the AP and within its antenna directions, while diminishing in more distant or obstructed areas. When considering the RSS maps of both Wi-Fi and 5G together, 5G signals can provide broader and more consistent coverage, whereas high-band Wi-Fi excels in delivering exceptionally high-speed connectivity in specific regions. These results demonstrate that 5G can complement Wi-Fi technology to enhance overall in-building coverage.

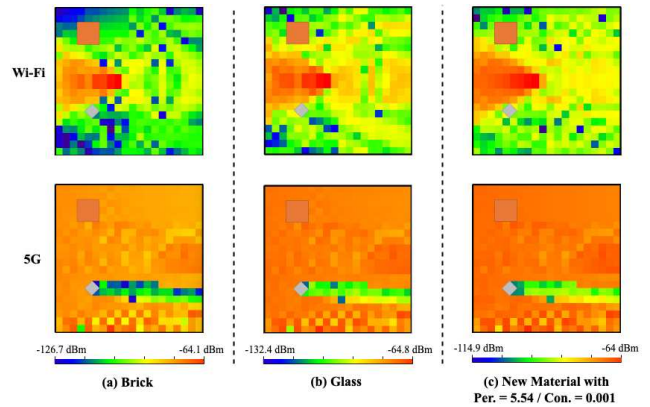


Fig. 2: RSS distribution maps with different wall materials.

On the other hand, we also conduct evaluation of RSS maps that vary in response to different wall materials. The results reveal that substituting brick walls with glass walls leads to enhancements in both 5G and Wi-Fi RSS. Furthermore, by fine-tuning material properties such as permittivity and conductivity, it becomes feasible to further enhance wireless coverage. It is observed an average increase of 40% and 33% in 5G and Wi-Fi RSS, respectively, when employing a novel material versus traditional materials. These findings have instilled motivation for the development of a framework aimed at predicting the optimal building material for customized network coverage across diverse environmental configurations, which is the subject elaborated upon in the subsequent section.

## III. GEMNET: MATERIAL-INSPIRED NETWORK PLANNING

In this section, we first introduce the ray-tracing analysis to generate large volumes of training data for our *GemNet* model. We then explore data preprocessing and present two distinct graph-based models designed for predicting optimal material properties to meet specific network coverage requirement.

### A. Data Acquisition

In a bid to elucidate the correlation between the material properties of building walls and RSS distribution maps, we amass a dataset including over 10,000 entries using *Wireless Insite*®. The dataset is publicly available at [12]. Each entry contains a particular wall material's conductivity and permittivity, accompanied by corresponding heatmaps illustrating the

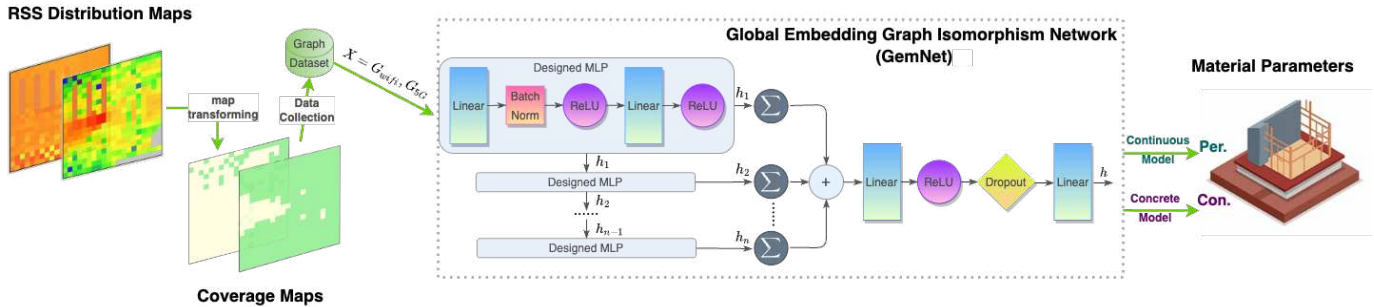


Fig. 3: Overview of the GemNet prediction model.

distribution of Wi-Fi and 5G signal strength at each grid location (referred to as a *node*) within indoor environments.

Specifically, these heatmaps included in the dataset provide detailed information regarding signal strength of multiple direct and reflection paths at various spatial coordinates. This information aids in identifying crucial points, such as areas with strong or weak signals, trajectories with the highest RSS, and locations where signal boost is possible. Also, we perform data augmentation to represent each heatmap in the form of a *graph*. Converting the heatmap into a graph format enables GNN algorithms use to identify RSS distribution patterns and understand the correlations among different crucial points within the space (see more details in Sec. III-C). Thus, the dataset comprises five attributes totally, including material conductivity, permittivity, Wi-Fi heatmap, 5G heatmap, and the adjacency matrix of the transformed graph.

#### B. From RSS Distribution to Binary Coverage Maps

Next, we implement a series of preprocessing steps to the raw data, transforming the acquired heatmaps into comprehensive signal coverage maps. This transformation involves converting the heatmap into a binary signal coverage map because, in practice, what matters most to users is the presence or absence of a signal in their immediate vicinity, rather than the exact numerical signal strength. For both 5G and Wi-Fi signals, a predefined threshold distinguishes strong from weak signals, where signals exceeding this threshold are considered available, while those below it are deemed unavailable. This transformation is necessary to create a more coarse-grained signal coverage map. Comparatively, when used as input for predicting optimal material properties as in the subsequent subsection, the binary signal coverage map offers sufficient information, encompassing the indoor topological structure and RSS variations, to facilitate model learning.

Specifically, RSS is influenced by various factors, including architectural structures, object layouts, device placements, and potential sources of interference. When considering RSS in a holistic manner and utilizing the RSS Indicator (RSSI) as the evaluation metric, signal quality within indoor environments can be categorized as, e.g., Excellent (-50dBm to -70dBm), Acceptable (-70dBm to -80dBm), Weak (-80dBm to -90dBm), Virtually Unusable (below -90dBm). Depending on the network requirements, minimum acceptable RSS thresholds, denoted as  $T_{5G}$  and  $T_{wifi}$ , can be chosen for

5G and Wi-Fi RSS maps. The original signal strength for each node  $i$  is set as  $S_{5G,i}$  and  $S_{wifi,i}$ . To represent the 5G and Wi-Fi coverage maps, we use the matrices  $B_{5G}$  and  $B_{wifi}$ , where each element corresponds to a binary value at the respective node on the map. If there are  $n$  nodes, then each matrix contains  $n$  elements, signifying the binary value of a node. This way, the 5G binary coverage map can be defined as  $B_{5G} = [B_{5G,1}, B_{5G,2}, B_{5G,3}, \dots, B_{5G,n}]$  and the Wi-Fi binary coverage map is expressed as  $B_{wifi} = [B_{wifi,1}, B_{wifi,2}, B_{wifi,3}, \dots, B_{wifi,n}]$ , where

$$B_{5G,i} = \begin{cases} 1 & \text{if } S_{5G,i} > T_{5G} \\ 0 & \text{if } S_{5G,i} \leq T_{5G}, \end{cases} \quad (1)$$

$$B_{wifi,i} = \begin{cases} 1 & \text{if } S_{wifi,i} > T_{wifi} \\ 0 & \text{if } S_{wifi,i} \leq T_{wifi}. \end{cases} \quad (2)$$

These binary coverage maps will be employed as input data for the subsequent graph-based learning model used to predict optimal material parameters.

#### C. GemNet: Global Embedding Graph Isomorphism Network

The Graph Isomorphism Network (GIN) represents a variation of the GNN model and is distinct from conventional approaches such as the Graph Convolution Network or Graph Attention Network, which are typically used for node-level classification. GIN, on the other hand, is well-suited for tasks involving graph-level classification or regression. In this work, we employ 5G and Wi-Fi binary coverage maps as inputs, leveraging an extended GIN model to predict desired material parameters, namely permittivity and conductivity, in order to meet the coverage demands. Utilizing GIN as the foundation for our approach proves to be highly suitable for two reasons:

- *Node Feature Capturing*: In our signal coverage map, Each node represents a reception point with features such as RSS and positional data. The GIN model, through iterative processes, captures spatial correlation based on the environment layout. Thus, embedded nodes can indirectly learn information from more distant neighbors while integrating them into the graph's structure as illustrated in Sec. III-A.
- *Graph Isomorphism Discrimination*: Since the data is collected under a consistent configuration, the input binary coverage maps share a degree of similarity in topology

and signal propagation patterns. The incorporated Multilayer Perceptron Layers within the GIN model (MLP) can easily capture these subtle feature variations, enabling it to learn node attributes and their combinations. This means that, even if two graphs are structurally isomorphic, as long as their node features differ, the model can naturally distinguish between them.

1) *One Aggregator to ‘Rule Them ALL’*: In the model structure, illustrated in Fig. 3, our approach incorporates a unique layer termed *global pooling*, which stands in contrast to the GNN-based approach of exclusively learning node embeddings. This novel layer combines node embeddings to produce a comprehensive graph-level embedding. Such a concept draws inspiration from the discriminative capabilities of the Weisfeiler-Lehman graph isomorphism (W-L) test. To maximize the power of network representation, an aggregator, as seen in [13], is designed within our GemNet model to generate distinct node embeddings when dealing with non-isomorphic graphs for the efficacy of W-L test. The key to this solution lies in approximating two injective functions, predicated on the Universal Approximation Theorem and employing MLPs. To be specific, the hidden vector for a node  $i$  is computed as follow:

$$h_i = \mathcal{M} \left( (1 + \varepsilon)x_i + \sum_{j \in \mathcal{N}_i} x_j \right). \quad (3)$$

In Eq. (3),  $\mathcal{M}$  is an MLP, and  $\varepsilon$  quantifies the relative significance of the target node  $x_i$  compared to its neighbors  $x_j$ . It is worth noting that the reference to  $\mathcal{M}$  underlines the necessity for multiple layers (typically more than three), which are considered adequate for a comprehensive graph learning.

2) *Global Pooling*: To thoroughly analyze all structural information, especially when distinguishing entire 5G and Wi-Fi RSS graphs, it is imperative to employ global pooling or graph-level readouts. This approach generates a *unified* graph embedding from the individual node embeddings. Typically, global pooling can be realized through one of three common methods, each producing a distinct graph embedding, denoted as  $h_G$ , involving the mean, summation, or maximum of each node embedding  $h_i$ :

$$h_{G_\mu} = \frac{1}{N} \sum_{i=1}^N h_i, \quad h_{G_S} = \sum_{i=1}^N h_i, \quad h_{G_M} = \max_{i=1}^N (h_i). \quad (4)$$

The summation operator  $h_{G_S}$  shown in Eq. (4) exhibits a notable increase in expressiveness compared to the mean and max operators. This heightened efficacy is attributed to its ability to retain embeddings from preceding layers, where the embeddings are summed and the result is concatenated. This innovative approach combines the inherent expressive power of the summation operator with the memory enhancement provided by the concatenation of previous iterations. Based on these insights, the global pooling method is derived as:

$$h_G = \sum_{i=0}^N h_i^0 \parallel \cdots \parallel \sum_{i=0}^N h_i^k \quad (5)$$

In this context, each inclusion of structural information emphasizes the ability to precisely differentiate between the 5G and Wi-Fi RSS graphs. This, in turn, enhances our comprehension of the underlying patterns and variances within the data.

3) *Continuous Model for Permittivity Prediction*: The model design for the prediction of dielectric material parameters – permittivity and conductivity, is slightly different depending on their data distribution properties. First, permittivity (often represented as relative permittivity  $\varepsilon_r$ ) values typically span a continuous range from 1 to 10, encompassing various specific materials. Hence, predicting permittivity can be framed as a regression problem and addressed with a continuous learning model. Through a fine-tuning process, we construct the model consisting of several MLPs that begin with a linear fully connected layer (FC), followed by a batch normalization layer (BN) and another FC layer with activation functions ReLU. This process is formulated as:

$$\mathcal{M}(x) = \text{ReLU}\{W_2 \cdot (\text{ReLU}[BN(W_1 x + b_1)] + b_2\}, \quad (6)$$

where  $W_1$  and  $b_1$  are the weight and bias of the first linear layer, and  $W_2$  and  $b_2$  correspond to those of the second linear layer. Algorithm 1 summarizes the generalized GemNet modeling process. This algorithm begins with the extraction of input data (line 4), followed by a node embeddings section (lines 5-7), where the algorithm iteratively processes each layer using a convolution function to compute the node embeddings. Next, the graph-level embeddings  $h_l$  are computed for each layer (lines 8-10), which are then concatenated into a comprehensive graph embedding  $h$  (lines 11-12); Lastly, a dropout layer combined with the linear transformation are used to get the final graph embedding output (lines 13-17).

4) *Discrete Model for Conductivity Prediction*: In contrast to permittivity, the conductivity ( $\sigma$ ) of dielectric materials exhibit a wide range of values, typically in the low-value spectrum, spanning from approximately  $10^{-3}$  to  $10^{-15}$  S/m. Especially when considering building materials, based on the classification of electrical conductivity, they can be roughly categorized into three groups: poor dielectric materials (like metal-reinforced multilayer composite materials), general dielectric materials (such as ceramic, glass, and rubber composite materials), and good dielectric materials (including certain special plastics and high-purity quartz). Consequently,  $\sigma$  is distributed *discretely* based on the specific type of material in use. As such, we add a discretization layer to Algorithm 1 to map the original  $\sigma$  value to a set of class values  $c$  (e.g., ranging from 0 to 118), which can effectively capture the variance through our loss function. Subsequently, when calculating the model accuracy, we map  $c$  back to  $\sigma$ , as shown in Eq. (7).

$$c = f(\sigma) = \lfloor \text{scale} \cdot \sigma \rfloor \quad (7a)$$

$$\sigma = f^{-1}(c) = \frac{c}{\text{scale}}, \quad (7b)$$

where  $\text{scale}$  is an appropriate scaling factor. To summary, the entire GemNet process allows for the prediction of required building material properties based on the input of customized coverage maps.

**Algorithm 1** Generalized GemNet Model

```

1: Input:
  data :  $\{x, edge\_index, batch\}$ 
  L : number of layers
  GemNetConv( $h, edge\_index$ ) : GIN convolution layers
2: Output:
   $h$  : the final output of graph embedding ( $\varepsilon_r, \sigma$ )
3: Procedure:
4: a. Extract  $x$ ,  $edge\_index$ , and  $batch$  from data
5: b. Node Embeddings
6: for  $l = 1$  to  $L$  do
  Compute:  $h_l = \text{GemNetconv}(h_{l-1}, edge\_index)$ 
  where  $h_0 = x$ 
7: end for
8: c. Graph-level Readout
9: for  $l = 1$  to  $L$  do
  Compute:  $h_l = \text{global\_add\_pool}(h_l, batch)$ 
  based on the sum operator in Eq. (4)
10: end for
11: d. Concatenate graph embeddings
12: Concatenate all computed  $h$ 's based on Eq. (5):
   $h = \text{concat}(h_1, h_2, \dots, h_L, \text{dim} = 1)$ 
13: e. Regressor
14: Compute:  $h = \text{ReLU}(\text{lin1}(h))$ 
15: Apply dropout to  $h$ :  $h = \text{Dropout}(0.5, h)$ 
16: Compute the final output:  $h = \text{lin2}(h)$ 
17: Return  $h$ 

```

**IV. IMPLEMENTATION AND EVALUATION RESULTS**

In this section, we evaluate the performance of our GemNet prediction model, specifically examining its precision and stability under various network scenarios.

**A. Network Settings**

We consider network scenarios in which indoor devices can receive signals from either outdoor 5G BS or indoor Wi-Fi AP. *Wireless Insite®* is utilized to create realistic indoor scenarios by placing random objects on the floor. Specifically, the floorplan with dimensions 20m x 20m x 3m is designed to closely resemble an office environment, incorporating objects of varying heights and a range of placement densities, from sparse to dense. The material of the left outer wall is varied as the experimental parameter across different value sets, while the rest of the exterior walls, floor, and ceiling are consistently constructed with concrete material. Besides, Wi-Fi APs (60 GHz) are strategically located at the center of the room, while the 5G BS (sub-6 GHz) is deployed 50m away from the building's exterior. The entire area is divided into a  $20 \times 20$  grid of receivers, each covering an equal area of  $1 \text{ m}^2$ , in order to capture and visualize the RSS levels at different locations.

**B. Prediction Accuracy of Material Properties**

To validate the effectiveness of our proposed GemNet model, we divided the dataset, consisting of more than 20,000 data points, into training and test sets in a 90% to 10%

ratio. In practice, the material parameters can vary slightly due to factors like temperature and atmospheric pressure over the course of the day. Based on the actual measurements from prior study [14], a prediction error within 10% when compared to the ground truth is always considered reasonable. Hence, we adopt the Error Tolerance Rate (ETR) to assess prediction accuracy, where the predicted values of  $\varepsilon_r$  and  $\sigma$  are considered accurate when the percentage difference from the ground truths falls below the ETR of 0.1.

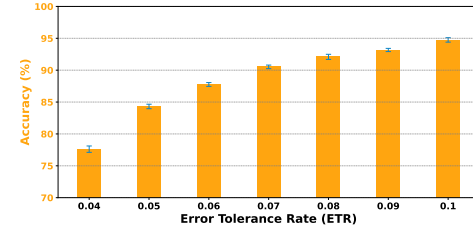


Fig. 4: Prediction accuracy vs. ETR.

Fig. 4 shows the correlation between ETR and the prediction accuracy of  $(\varepsilon_r, \sigma)$ . As ETR increases from 0.04 to 0.1, the model's prediction accuracy also rises, reaching approximately 77.61% to 94.75%. Notably, at an ETR of 7%, consistent with the acceptable error range described in [14], the model achieves an accuracy of 90.52%. This indicates that our GemNet predictions are generally highly accurate, confirming its validity and practical utility.

**C. Model Consistency and Generalization**

To further evaluate the performance of GemNet and make informed decisions regarding model parameters, we conduct an analysis of the loss function's convergence during the training process. This analysis provides insights into the GIN-based model's ability to learn the underlying patterns and regularities within the collected data.

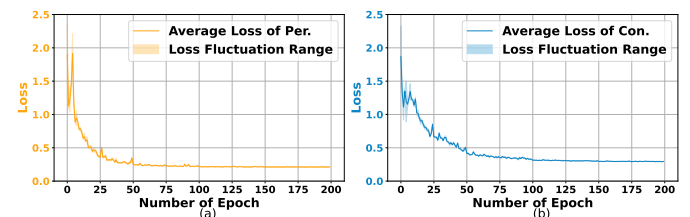


Fig. 5: Convergence on (a) permittivity and (b) conductivity model training.

In Fig. 5, we can observe the variations in the loss function as the number of training epochs increases. Fig. 5(a) and Fig. 5(b) depict the convergence of the loss function for training the continuous model and discrete model for  $\varepsilon_r$  and  $\sigma$ , respectively. During the initial 100 epochs, the fluctuations in the loss values suggest that the models are rapidly learning and adjusting. Subsequently, as the loss values stabilize, it indicates that both models have reached a local optimum, with learning and adjustments slowing down, signifying convergence. The

stability within the shaded area underscores the robustness of GemNet and its ability to generalize effectively to unseen data.

#### D. Analysis of Performance Margin

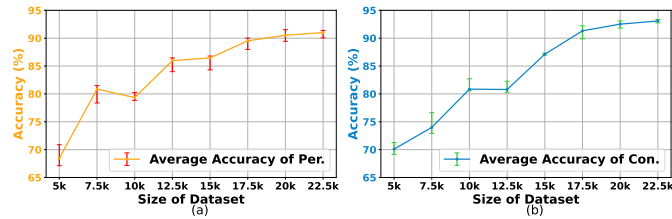


Fig. 6: Prediction accuracy on (a) permittivity and (b) conductivity vs. the amount of training data.

In this section, we explore the impact of dataset size on prediction performance, given an ETR of 0.07. As shown in Fig. 6, increasing the dataset size leads to improved accuracy for both continuous and discrete models. Particularly, as the dataset grows from 5,000 to 20,000, we observe a significant enhancement in model accuracy. However, as the dataset size continues to increase, the rate of accuracy improvement gradually diminishes, indicating a trend of *diminishing marginal returns*. This analysis suggests that a dataset of approximately 20,000 entries effectively reaches the performance boundary and fulfills the data requirements of the GemNet model.

#### E. Case Study for Practitioner using GemNet

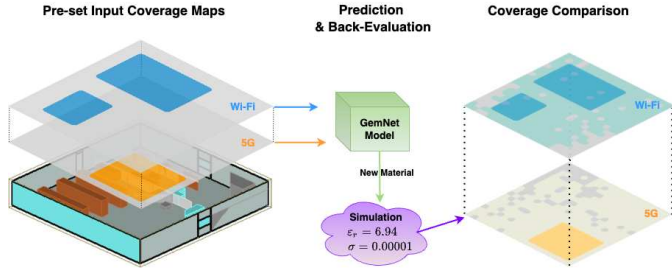


Fig. 7: Workflow of case study and results.

This case study aims to validate the practicality of the GemNet model within preset network coverage areas. Initially, specific areas requiring 5G and Wi-Fi services were designated based on scenario requirements. As illustrated in Fig. 7, the office scenario features a yellow area designated for public visitors, which demands 5G connectivity services to ensure the personal data communication. Meanwhile, the blue area serves as the workspace, where Wi-Fi services are required for local employees to access the internet. Subsequently, the corresponding binary coverage maps are fed into the pre-trained GemNet model, producing new material parameters customized to meet the prior coverage demands. To validate the feasibility of these material parameters, we then conduct an experiment using the same environment from the original data collection. The results in Fig. 7 show that the in-building coverage achieved with these predicted material parameters not only meets but also exceeds the initial coverage requirements. For instance, in the 5G coverage map, the light yellow area

in the right figure represents the indoor network coverage achieved using the new predicted materials, and it effectively covers the original preset dark yellow area in the left figure.

## V. CONCLUSION AND FUTURE WORKS

This paper elucidated the crucial relationship between building material properties and the distribution of indoor wireless signals, laying the foundation for the material-inspired networking design to foster tailored network services. Through a comprehensive analysis, we showed the significant impact of wall material characteristics on wireless signal propagation. Then, the novel dataset generated through ray-tracing analysis served as the foundation for a GIN-based predictive model. This model, boasting over 90% accuracy in predicting material parameters based on network coverage demands, emerges as a promising tool for optimizing indoor wireless environments.

In future work, we will consider additional factors influenced by material properties, such as noise reduction and thermal insulation, to establish a holistic ecosystem that accommodates various applications. Besides, material strength and cost will be considered, helping to refine the selection of suitable material parameters for optimizing network performance.

## ACKNOWLEDGEMENT

This research was supported by the National Science Foundation through Award CNS-2312138 and CNS-2312139.

## REFERENCES

- [1] B. Feng and C. Zhang et al., "D2D communications-assisted traffic offloading in integrated cellular-wifi networks," *IEEE IoT Journal*, 2019.
- [2] Y. Jian, Y. Liu, S. K. Venkateswaran, D. M. Blough, and R. Sivakumar, "A quantitative exploration of access point mobility for mmwave wifi networks," in *IEEE International Conference on Communications*, 2020.
- [3] M. Chen, D. Gündüz, K. Huang, W. Saad, M. Bennis, A. V. Feljan, and H. V. Poor, "Distributed learning in wireless networks: Recent progress and future challenges," *IEEE Journal on Selected Areas in Communications*, vol. 39, no. 12, pp. 3579–3605, 2021.
- [4] W. C. Stone, "Electromagnetic signal attenuation in construction materials," 1997.
- [5] A. Aileen, A. D. Suwardi, and F. Prawiranata, "Wifi signal strength degradation over different building materials," *Engineering, Mathematics and Computer Science (EMACS) Journal*, vol. 3, no. 3, 2021.
- [6] A. Asp, Y. Sydorov, M. Keskkastari, M. Valkama, and J. Niemela, "Impact of modern construction materials on radio signal propagation: Practical measurements and network planning aspects," in *IEEE Vehicular Technology Conference (VTC Spring)*, 2014, pp. 1–7.
- [7] A. Hussien, W. Khan, A. Hussain, P. Liatsis, A. Al-Shamma'a, and D. Al-Jumeily, "Predicting energy performances of buildings' envelope wall materials via the random forest algorithm," *Journal of Building Engineering*, vol. 69, p. 106263, 2023.
- [8] O. A. Tafreshi, Z. Saadatnia, and S. Ghaffari-Mosanenzadeh et al., "Machine learning-based model for predicting the material properties of nanostructured aerogels," *SPE Polymers*, vol. 4, no. 1, 2023.
- [9] H. Zuo et al., "Prediction of properties of metal alloy materials based on machine learning," *arXiv preprint arXiv:2109.09394*, 2021.
- [10] P. Zhang, C. Yi, B. Yang, and C.-X. Wang et al., "In-building coverage of millimeter-wave wireless networks from channel measurement and modeling perspectives," *Science China Information Sciences*, 2020.
- [11] H. Sun, H. V. Burton, and H. Huang, "Machine learning applications for building structural design and performance assessment: State-of-the-art review," *Journal of Building Engineering*, vol. 33, p. 101816, 2021.
- [12] Z. Yang. Dataset for GemNet prediction model. [Online]. Available: <https://github.com/zhijin44/Dataset-for-GemNet-prediction-model>
- [13] K. Xu, W. Hu, J. Leskovec, and S. Jegelka, "How powerful are graph neural networks?" *arXiv preprint arXiv:1810.00826*, 2018.
- [14] J. Qin, Z. Liu, M. Ma, and Y. Li, "Machine learning approaches for permittivity prediction and rational design of microwave dielectric ceramics," *Journal of Materiomics*, vol. 7, no. 6, pp. 1284–1293, 2021.